

Results from a Hidden Photon Dark Matter Search Using a Multi-Cathode Counter

A. Kopylov,¹ I. Orekhov, V. Petukhov

Institute for Nuclear Research RAS,
prospect 60-letiya Octyabrya 7a, Moscow 117312, Russia

E-mail: beril@inr.ru

Abstract. Here we present measurements of the rates of emission of single electrons from the cathode of a proportional counter filled with a mixture of Ar + CH₄ (10%) at 1 bar. We interpret the results as a possible photoelectric effect associated with hidden photons (HPs). Our results set upper limits for HPs from cold dark matter (CDM). We also discuss future options for searches for HPs from CDM using a multi-cathode counter technique.

¹Corresponding author.

Contents

1	Introduction	1
2	Measurement strategy	1
3	Apparatus	2
4	Data analysis	4
5	Summary	5

1 Introduction

To advance experimental efforts in the search for dark matter, physicists are now looking for new approaches. One such approach is to use a dish antenna to observe hidden photons (HPs) from cold dark matter (CDM) [1]. This technique has placed an upper limit on the HP mass of $m_{\gamma'} = 3.1 \pm 1.2$ eV [2]. This range of masses is limited by the coefficient of reflection of light from the mirror and by the spectral sensitivity of the photomultiplier tube. At higher frequencies, the light is absorbed by the reflecting surface, which results in a loss of sensitivity for this technique. However, the absorption of higher-frequency light causes the emission of electrons from the surface if the photon energy is higher than the work function of the metallic reflector. Hence, by counting single electrons emitted from the metal one can extend the sensitivity of this technique into the vacuum ultraviolet range and higher.

We have developed a special detector for this study—a multi-cathode counter [3]—and we have previously reported the first results of measurements using a counter with a copper cathode [4]. We have used a new counter of improved design, which employs an aluminium cathode and focusing rings, to make measurements with increased sensitivity [5]. Here we summarise the results of all of our measurements and outline our plans for further research.

2 Measurement strategy

If dark matter is composed entirely of HPs, then the power collected by a detector (here, by a cathode of the counter) is

$$P = 2\alpha^2\chi^2\rho_{CDM}A_{cath} \quad (2.1)$$

where $\alpha = \cos(\theta)$ and θ is the angle between the direction of the HP field, when it points in the same direction everywhere, and the surface of the cathode, with $\alpha^2 = 2/3$ if the HP vector is distributed randomly; $\rho_{CDM} \approx 0.3\text{GeV}/\text{cm}^3$ is the energy density of CDM, which we assume to be equal to the energy density of the HPs; A_{cath} is the area of the cathode of the counter; and χ is a dimensionless parameter that quantifies the kinetic mixing as it is explained in [1]. If this power is converted into single electrons that are emitted from the cathode of the counter, then

$$P = m_{\gamma'} \cdot R_{MCC}/\eta \quad (2.2)$$

where $m_{\gamma'}$ is the mass (energy) of an HP, η is the quantum efficiency for a photon with energy $m_{\gamma'}$ to yield a single electron from the surface of the metal, and R_{MCC} is the rate at which single electrons are emitted from the cathode, which is presumed here to be entirely due to HPs. Thus, by combining (2.1) and (2.2) we obtain:

$$\chi_{\text{sens}} = 2.9 \cdot 10^{-12} \left(\frac{R_{MCC}}{\eta \cdot 1Hz} \right)^{\frac{1}{2}} \left(\frac{m_{\gamma'}}{1eV} \right)^{\frac{1}{2}} \left(\frac{0.3 \text{ GeV/cm}^3}{\rho_{CDM}} \right)^{\frac{1}{2}} \left(\frac{1m^2}{A_{MCC}} \right)^{\frac{1}{2}} \left(\frac{\sqrt{2/3}}{\alpha} \right) \quad (2.3)$$

Here we assume the quantum efficiency η for the conversion of the HP at the surface of the metal cathode to be equal to the quantum efficiency for a real photon of the same energy. The sensitivity depends critically upon the dark rate of the counter. Single electrons can be emitted by defects on the surfaces of the wires, by protrusions, and by heterogeneous spots on the surface of the cathode. Given these conditions, the value of χ obtained from (2.3) is only an upper limit. To improve the limit, we need to decrease the dark rate of the counter. One way to accomplish this would be to apply a surface treatment to diminish the effects of extraneous sources. Another possibility would be to lower the temperature of the detector to diminish the contribution from thermionic emission, which depends on the work function ϕ_W of the metal and the temperature T in Kelvins, as expressed by the Richardson equation:

$$R_{\text{therm}} = a \cdot T^2 \cdot e^{-\frac{\phi_W}{kT}} \quad (2.4)$$

where R_{therm} is the thermionic dark rate, a is a constant, and k is Boltzmann's constant. Using an Ar/CH_4 mixture enables us to lower the temperature to $-40^\circ C$, which can substantially reduce the thermionic dark rate.

3 Apparatus

Figure 1 shows a schematic illustration of a multi-cathode counter. The counter is filled with an $Ar + CH_4$ (10%) mixture at 1 bar. It has three cathodes and one anode made of gold-plated tungsten-rhenium wire $25 \mu m$ in diameter. We apply the low (negative) potential HV1 to cathode 1, the outer cathode, which is fabricated from a metallic sheet, and we measure the counting rate of individual electrons emitted from the surface of this sheet. The second cathode is placed 5 mm from the outer cathode. It consists of a series of nichrome wires $50 \mu m$ in diameter, with a pitch of 4.5 mm. This cathode serves as a barrier to the electrons emitted from outer cathode. We apply the potential HV2 to cathode 2. In configuration 1, HV2 is higher than HV1, so that electrons emitted from cathode 1 can drift to the central counter with the still-smaller-diameter cathode 3, which is made of nichrome wires $50 \mu m$ in diameter, with a pitch of 6 mm. The smaller (40 mm) diameter of cathode 3 is used to obtain the high ($\approx 10^5$) gas amplification needed to register the signal from single electrons. In configuration 2, the potential HV2 is lower than HV1, so that electrons emitted from the outer cathode are scattered back from cathode 2 and do not reach the central counter. We use this configuration

to measure the dark rate due to electrons emitted from the wires and to ionising particles that cross the counter along short tracks at both ends. The two configurations have similar geometries and similar electric fields, so we expect that the difference $R_1 - R_2$ between the count rates measured in these two configurations measures the net effect due to electrons emitted from the outer cathode.

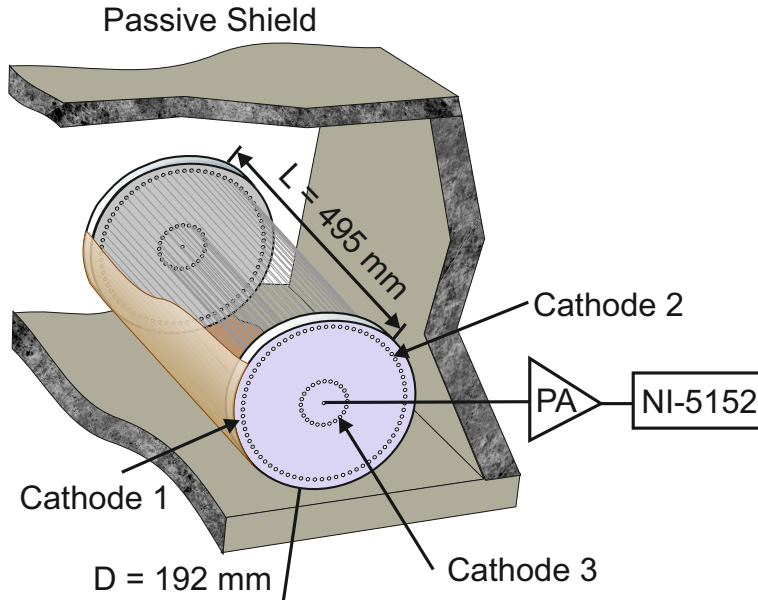


Figure 1. Schematic view of the multi-cathode counter in the shielded cabinet.

To reduce the background due to gamma radiation from the surrounding walls, we placed the counter in a special cabinet made of steel slabs 30 cm thick. We have measured the γ -ray spectrum both inside and outside the shielding with a NaI(Tl) detector and the attenuation was obtained by comparing the two spectra. The attenuation of the gamma radiation by the shielding was greater than a factor of 100 for gamma rays at the ≈ 200 keV peak energy of the gamma-spectrum measured by a NaI(Tl) crystal. Measurements with the copper counter showed that with the counter placed outside the shield the count rate for single electrons was about 20% higher than the one obtained inside the shield. From here, we found that for the copper counter inside the shield the contribution to the single-electron count rate due to gamma radiation is less than 0.2% of the single-electron count rate. The given estimation of the remaining contribution from ambient gammas is a rough one like an order estimation. No events have been observed coincident with muons crossing the detector. The rate R_{MCC} is obtained here as the difference $R_1 - R_2$ between the count rates in the two configurations, with different potentials at the second cathode [3]; see Figure 1. We assume that in configuration 1, the count rate is determined by the rate of emission of single electrons from the cathode of the counter, the wires and particles with short tracks crossing the counter at both ends (the end effect). In configuration 2, the rate is determined by the rate of emission from the wires and the end effect. The exact contributions of the end effect and the wires to the total count rate in configuration 2 is unknown for this technique. This uncertainty is the main source of our systematic error.

We estimated the number of electrons lost during diffusion from the outer cathode of the counter to the central counter based on the attachment mechanism proposed by Bloch and

Bradbury and developed by Herzberg (BBH model) [6, 7] for electrons of small energies. The number of free electrons in a gas that contains electronegative impurities (in our case, oxygen impurities) decreases exponentially:

$$N(t) = N(0) \cdot e^{-At} \quad (3.1)$$

where $N(t)$ is the number of electrons at time t , $N(0)$ is the initial number of electrons, and A is the attachment rate. The latter is given by the expression

$$A = P(M) \cdot P(O_2) \cdot C_{O_2,M} \quad (3.2)$$

where $P(M)$, $P(O_2)$ are the pressure of the working gas and of oxygen, respectively, and $C_{O_2,M}$ is the coefficient of attachment, which does not depend upon the pressure of the gas or the impurities in the BBH model.

The field strength in our detector, as calculated using Maxwell16, is presented in figure 2.

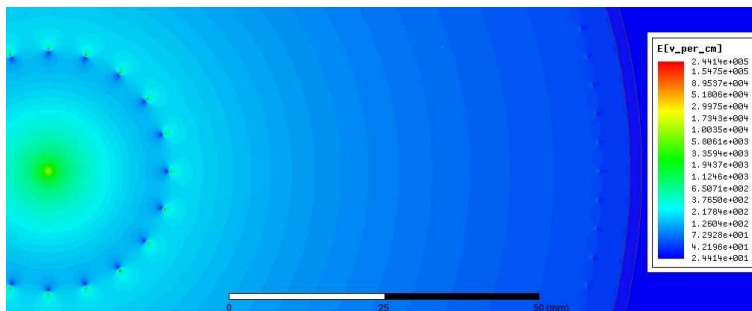


Figure 2. The calculated electric-field strength across the counter.

Using data for the dependence of the drift velocities of the electrons upon E/p in the argon-methane mixture [8] and for the coefficient of attachment $C_{O_2,M}$ from [9], one can determine the probability for an electron to become attached while drifting from the outer cathode to the central counter. We found that for our gas mixture this probability is less than 1%; *i.e.* it can be neglected.

4 Data analysis

We digitised the pulse shapes in intervals of ± 50 mV at a frequency of 10 MHz and a sampling step of $400 \mu\text{V}$. Each measurement lasted for 12 h, after which we processed the data offline. To select “true” events, we performed a selection in the three-parameter space defined by the amplitude of the pulse, the duration of the leading edge of the pulse, and a parameter β that describes the prehistory of the event. The latter quantity is proportional to the first derivative of the baseline, which we approximated as a straight line during the $50 \mu\text{sec}$ before the leading edge of the pulse. We estimated the efficiency as the probability for the pulse to belong to the ROI box in this 3-parameter space; we found it to be $(88 \pm 6)\%$. To reduce the influence of noise on the counting, we selected only intervals with a baseline deviation not more than 5 mV from zero, taking into account a proper correction for the live time of the counting, which we found to be about 54%.

To evaluate the contribution to the total measured rate of the rate of emission of electrons from the wires, we need to consider that in configuration 2 only those parts of the surfaces of the wires that face the centre of the counter produce the effect. Electrons emitted from the opposite sides are retarded by the potential of the second cathode and cannot drift toward the central counter. They are thus trapped in the region between the first and second cathodes (figure 3). This reduces the background measured in configuration 2. Instead of $R_1 - R_2$, which is the appropriate value if the entire rate is due to the end effect, in the case where the entire rate is due to the wires we should use:

$$R_{MCC} = R_1 - \frac{n_3 + n_2}{n_3 + n_2/2} R_2 \quad (4.1)$$

Here n_2 and n_3 are the numbers of wires in the second and third cathodes, respectively, see [5].

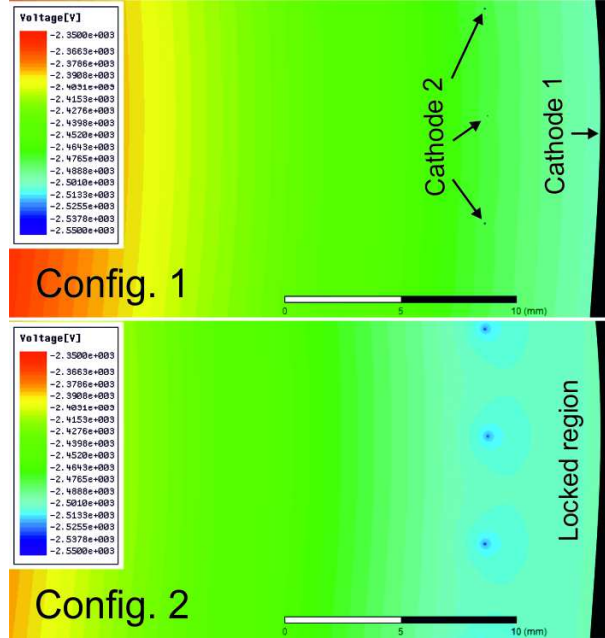


Figure 3. Calculated electric potentials across the counter for the two configurations.

5 Summary

In this section, we summarise the results of all our measurements, using $R_1 - R_2$ to evaluate the net event rate. We took the limit Cu-1 from the results in [4], which we obtained by using a counter with a copper outer cathode at room temperature. At the beginning of these measurements, we observed some instability in the counter, which resulted in large scattering of the experimental data points and consequently in large errors. This explains the relatively large uncertainty of these first measurements. Later measurements showed that after working continuously for about a month the instability disappeared. We obtained the result Cu-2 when the counter had stabilised after this prolonged period of continuous work.

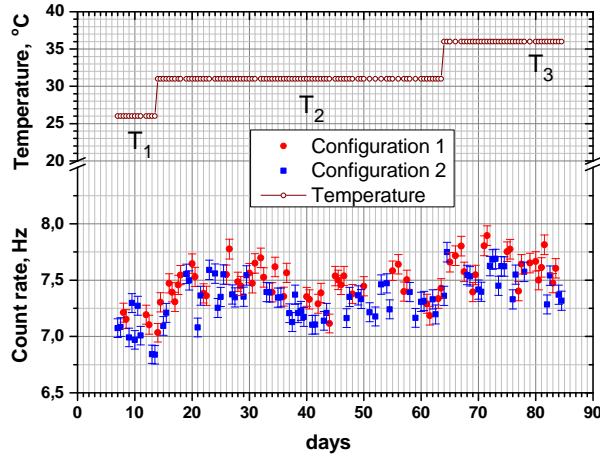


Figure 4. Results of measurements obtained using a counter with a copper cathode at different temperatures.

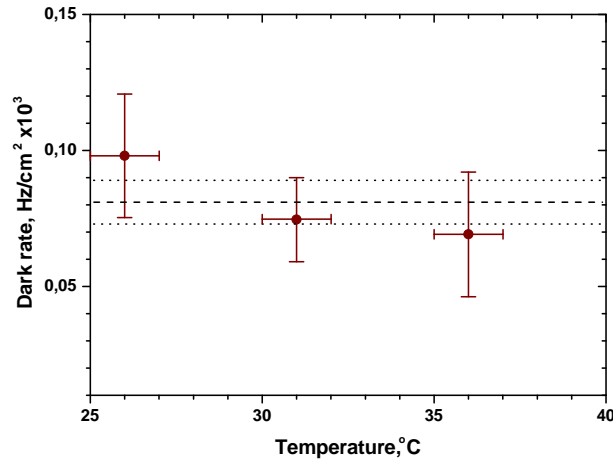


Figure 5. The distributions of events at 26°C, 31°C and 36°C. The dashed line is the average value obtained for all measurements, and the dotted lines represent $\pm 1\sigma$ levels from the average value.

After selecting for “true” pulses, we obtained for $r_{MCC} = R_{MCC}/A_{cath}$: $(0.98 \pm 0.22) \cdot 10^{-4} Hz/cm^2$, $(0.75 \pm 0.15) \cdot 10^{-4} Hz/cm^2$ and $(0.69 \pm 0.23) \cdot 10^{-4} Hz/cm^2$ for the temperatures 26°C, 31°C and 36°C, respectively (figure 5). The fact that the count rate does not exhibit a clear increase with temperature can be taken as evidence that there is a negligible contribution from thermionic emission. The average value obtained for all these temperatures is $r_{MCC} = (0.81 \pm 0.08) \cdot 10^{-4} Hz/cm^2$.

We obtained the limit Al-1 from the measurements presented in figure 6, where we assumed that the main contribution to the rate is due to the end effect.

The average value found for all the measurements presented in figure 6: $r_{MCC} = (0.8 \pm$

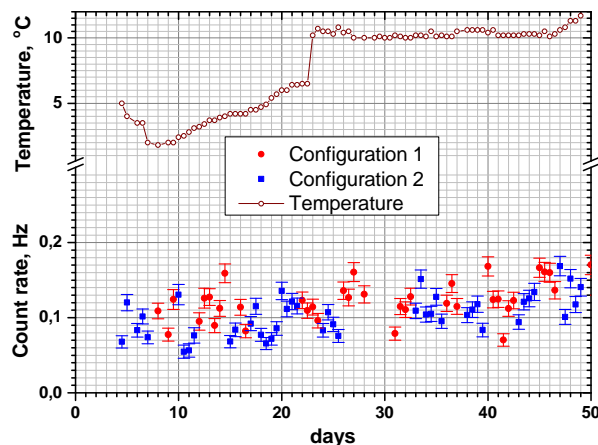


Figure 6. Results of measurements obtained using a counter with an aluminium cathode.

$0.25) \cdot 10^{-5} \text{ Hz/cm}^2$. This is the lowest result obtained to date.

The limits obtained at a 95% confidence level (CL) are presented in figure 7. Using (4.1) to account for the systematic uncertainties would substantially decrease the limits presented in this figure. The question of the relevant systematic uncertainty is now under further study. If we were to assume that electrons emitted from the cathode wires also contribute to the count rate, *i.e.* if we were to take into account our systematic errors, the curves for Cu-1, Cu-2 and Al-1 in figure 7 would be lower. An advanced surface treatment could further improve the sensitivity of the measurements.

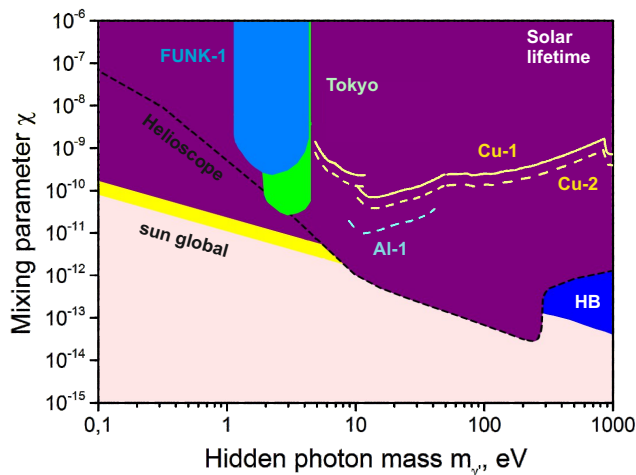


Figure 7. Limits at a 95% CL obtained from the series of measurements Cu-1, Cu-2 and Al-1. Here the Tokyo limits are from [2] and the FUNK-1 limits from [10].

We have made good progress using a counter with an aluminium cathode. Further

improvements can be made by using Ni or Pt, which have higher work functions, for the cathode of the counter. Figure 7 shows that our limits are higher than the limits given by the solar lifetime, so we still need to make significant improvements to go beyond these limits. However one should also take into account possible uncertainties due to two relevant processes: the emission of hidden photons inside the Sun and the emission of electrons from the metal surfaces. There is also a significant difference between volume and surface detectors. In the former, HPs are presumed to be detected by their interactions with valence electrons, while in the latter, detection is due to the interaction with free electrons in the degenerate electron gas. Our detector is a surface detector, so the limits obtained by this technique are related to the interaction of HPs with the free electrons in the degenerate electron gas of the metal.

Acknowledgments

The work was funded by the Federal Agency for Scientific Organizations, Russia. The authors would like to thank Enago (www.enago.com) for the English language review.

References

- [1] D. Horns, J. Jaeckel, A. Lindner et al., *Searching for WISPy cold dark matter with a dish antenna*, *JCAP* **04** (2013) 016.
- [2] J. Suzuki, T. Horie, Y. Inoue, and M. Minowa, *Experimental search for hidden photon CDM in the eV mass range with a dish antenna*, *JCAP* **09** (2015) 42.
- [3] A.V. Kopylov, I.V. Orekhov, V.V. Petukhov, *A method to register hidden photons with the aid of a multi-cathode counter*, *Tech. Phys. Lett.* **42** (2016) 879
- [4] A.V. Kopylov, I.V. Orekhov, V.V. Petukhov, *On a Search for Hidden Photon CDM by a Multicathode Counter*, *Advances In High Energy Phys.* **2016** (2016) 2058372
- [5] A. Kopylov, I. Orekhov, V. Petukhov, *A multi-cathode counter in a single-electron counting mode*, *NIM A* **910** (2018) 164.
- [6] F. Bloch and N. Bradbury, *On the mechanism of unimolecular electron capture*, *Phys. Rev.* **48** (1935) 689.
- [7] A. Herzenberg, *Attachment of Slow Electrons to Oxygen Molecules*, *J. Chem. Phys.* **51** (1969) 4942.
- [8] Alan A. Sebastian and J.M. Wadehra, *Time-dependent behaviour of electron transport in methaneargon mixtures* *J. Phys. D Appl. Phys.* **38** (2005) 1577
- [9] M. Huk, P. Igo-Kemenes and A. Wagner, *Electron attachment to oxygen, water, and methanol, in various drift chamber gas mixtures*, *NIM A* **267** (1988) 107.
- [10] R. Engel, D. Veberič, C. Schäfer et al., *Search for hidden-photon Dark Matter with FUNK*, *arXiv:1711.02961v1 [hep-ex]*